

Full Length Research Paper

Resolving a complex seismic moment tensor into a series of simple double couple sources: A case of Turkey

Mehmet Utku

Department of Geophysical Engineering, Faculty of Engineering, Dokuz Eylül University, TR-35160, Buca-İzmir, Turkey.
E-mail: mehmet.utku@deu.edu.tr.

Accepted 11 April, 2011

The main goal of studying double couple sources in seismology is to obtain a complete description of the physics of the source. In other words, it is to describe the force system equivalent to physical mechanism in earthquake focus. Seismic moment tensor is a mathematical quantity defining the earthquake source. It characterizes all the information about the source. With this purpose, it describes the equivalent forces of a seismic source. Then, seismic moment tensor is a necessary and sufficient condition for the description of the physics of seismic sources. Theoretically, a seismic source may be composed of different force systems. Each force system describes an elementary source model. A double couple source is just one of them. Nevertheless, the double couple system of equivalent forces is the most appropriate model for most earthquakes. However, an earthquake may also be a non-double couple. In practice, there is some evidence that supports the theory of non-double couple earthquake source mechanism. Therefore, the following four source models are considered: i) General moment tensor, ii) Pure-deviatoric moment tensor, iii) A moment tensor characterizing the pull-apart rupture, iv) A moment tensor characterizing the listric fault model. Any moment tensor can be represented by a linear combination of different elementary sources. Consequently, each source model above is a complex source and defined by a moment tensor. These are considered as time-independent moment tensors. The first source is generated by an isotropic component, two strike-slip faults, two vertical dip slip faults, and a reverse fault. The second source is like the first source, but there is no isotropic part in this complex source. The third source is a complex source contributed with respect to specific proportion of two strike-slip faults and a normal fault. The analysis of complex moment tensors calculated for these three source models shows that each source has a non-double couple mechanism. Finally, the fourth source model is a linear combination of more than one normal fault, the dips of which are gradually decreasing with depth. Nevertheless, this complex source is a double couple. However, this evaluation is a result of a calculation only due to fault geometry. Thus, to assume double-couple for the earthquake source is an incomplete approximation since the complex source assumption also contains the deviation from double couple.

Key words: Earthquake source, equivalent body forces, moment tensor, complex source, fault plane solution, pull-a-part structure, listric normal fault, Turkish earthquakes.

INTRODUCTION

The equivalent body forces are defined by Burridge and Knopoff (1964). Gilbert (1970) introduced the seismic moment tensor for calculating the excitation normal modes of free oscillation of the earth. The concept of a seismic moment tensor has been defined as the volume integral of the stress drop. Knopoff and Randall (1970)

represented the equivalent forces by a linear vector dipole. Randall (1971) showed that seismic moment of a generalized dislocation is a tensor. Gilbert (1973) gave the moment tensor elements for an isotropic source, a shear dislocation and a compensated linear vector dipole. Buland and Gilbert (1976) designed a matched filtering

for seismic moment tensor. The concept of seismic moment tensor was further extended by Backus and Mulcahy (1976) and Backus (1977a, b). Moment tensor can be determined from free oscillations of the earth (Gilbert and Dziewonski, 1975), long-period surface waves (McCowan, 1976; Mendiguren, 1977; Aki and Patton, 1978; Kanamori and Given 1981, 1982; Nakanishi and Kanamori, 1982, 1984), and long-period body waves (Stump and Johnson, 1977; Strelitz, 1978, 1980, 1981; Fitch et al., 1980, 1981; Langston, 1981; Dziewonksi et al., 1981; Dziewonski and Woodhouse, 1983a, b; Ekström and Dziewonski, 1985; Jost and Herrmann, 1989; Kikuchi and Kanamori, 1991). Fitch et al. (1981) compared moment tensors from surface waves and body waves. The moment tensor can be decomposed into an isotropic and deviatoric component (Fitch et al., 1980; Jost and Herrmann, 1989), or a major and minor double couple (Ben-Menahem and Singh, 1981; Kanamori and Given, 1981; Jost and Herrmann, 1989), or an isotropic part (IP) and double couple (DC) and compensated linear vector dipole (CLVD) (Knopoff and Randall, 1970; Ben-Menahem and Singh, 1981; Jost and Herrmann, 1989). Besides this, a complete moment tensor can be the superposition of an isotropic component and three vector dipoles (or three CLVD's or three double couples, Ben-Menahem and Singh, 1981; Jost and Herrmann, 1989). The higher order solution of the 2 moment tensors has been implemented by Backus and Mulcahy (1976) and Backus (1977a, b), Stump and Johnson (1982), Dziewonski and Woodhouse (1983a). Also the time-dependent moment tensor solution has been implemented by Dziewonski and Gilbert (1974), Gilbert and Dziewonski (1975), Backus and Mulcahy (1976), Backus (1977a), Stump and Johnson (1977), Strelitz (1980), Sipkin (1982), Vasco and Johnson (1988). Non double-couple earthquakes and their characteristics had been studied by Kubas and Sipkin (1987), Sipkin (1986), Frohlich (1995, 1990), Batini et al. (1995) and Frohlich et al. (1989).

Wang and Herrmann (1980) and Herrmann and Wang (1985) presented expression for the 10 Green's functions required to describe the wave field due to an arbitrary point dislocation source and a point explosion buried in a plane layered elastic medium. (Bouchon, 1981) expressed the Green's function for an elastic layered medium as a double integral over frequency and horizontal wave number, who shows that for any time window, the wave number integral can be exactly represented by a discrete summation.

In this study, examples are given for the calculation of forward solution of the time-independent moment tensor elements. By these examples, both the basic seismic sources are considered and some tectonic structure types are investigated. Therefore, firstly, the moment tensors of elementary sources are calculated because of multiple source character. They are called "elementary moment tensors". Secondly, the complex moment

tensors are formed. The complex moment tensor is a mathematical quantity that defines a multiple source, and it contains both the equivalent force systems to physical mechanism on its focus and the orientation parameters and some physical parameters of the resultant faultings. Finally, both their major couple solutions and the equivalent body force systems describing the source are determined by the analysis of calculated complex moment tensors. In addition, their contribution percentage in the seismic source is also given.

CALCULATION METHOD

Generally, the moment tensor is a double integral of the moment tensor density on the fault plane. In this sense, a moment tensor is defined as (Backus and Mulcahy, 1976)

$$M_{ij}(t) = \int_{\Sigma} m_{ij}(r, t) \cdot d\Sigma \quad (1)$$

where Σ , $m_{ij}(r, t)$ and (r, t) show the fault plane, moment tensor densities and source coordinate as space (r) and time (t) , respectively. The moment tensor densities describe the seismic moment for each point (r, t) on the fault plane. As for the moment tensor which defines a point, seismic source can be written as

$$M_{ij} = M_0 (v_i n_j + v_j n_i) \quad (2)$$

where M_0 is the scalar seismic moment, v is the slip vector of the fault plane, and n is the normal vector of the fault plane (Day and Mclaughlin, 1991; Jost and Herrmann, 1989; Madariaga, 1983; Doornbos, 1988, 1982; Aki and Richards, 1980). Equation (2) is a moment tensor that is real, symmetric, and second rank. The opened explanations of Equation (2) in the Cartesian coordinate system are (Jost and Herrmann, 1989; Doornbos, 1988; Aki and Richards, 1980)

$$M_{xx} = -M_0 (\sin\delta \cos\lambda \sin 2\Phi + \sin 2\delta \sin\lambda \sin^2 \Phi) \quad (3a)$$

$$M_{yy} = M_0 (\sin\delta \cos\lambda \sin 2\Phi - \sin 2\delta \sin\lambda \cos^2 \Phi) \quad (3b)$$

$$M_{zz} = M_0 (\sin 2\delta \sin\lambda) \quad (3c)$$

$$M_{xy} = M_0 (\sin\delta \cos\lambda \cos 2\Phi + 0.5 \sin 2\delta \sin\lambda \sin 2\Phi) \quad (3d)$$

$$M_{xz} = -M_0 (\cos\delta \cos\lambda \cos\Phi + \cos 2\delta \sin\lambda \sin\Phi) \quad (3e)$$

$$M_{yz} = -M_0 (\cos\delta \cos\lambda \sin\Phi - \cos 2\delta \sin\lambda \cos\Phi) \quad (3f)$$

The Cartesian coordinate system (x, y, z) is defined as (north, east, down). In equations (3), Φ , δ , λ denote the strike, dip, and slip of the fault plane. Generally, an

arbitrarily orientated seismic source can be represented as the superposition of more than one differently orientated elementary source. Therefore,

$$\mathbf{M} = a_1 M_1 + a_2 M_2 + \dots + a_n M_n \tag{4}$$

can be written (Kikuchi and Kanamori, 1991; Jost and Herrmann, 1989). Here, M is the complex moment tensor which defines arbitrarily orientated general seismic source. a_i is the weight constant and M_i shows the elementary moment tensors. Thus, a complex moment tensor is a superposition of the weighted elementary moment tensors.

For the mechanism solution of the source of interest, the analysis of Eigen values – Eigen vectors of tensor M is made. So, the major couple solution of seismic source represented by tensor M and the contribution ratios of force systems, which are equivalent to physical mechanism on focus, are determined. To do this, the moment tensor is decomposed to the equivalent body forces. The equivalent body forces are the force components forming the seismic source. The explanations $a_i = (a_{ix}, a_{iy}, a_{iz})^T$ are the orthonormal Eigen vectors corresponding to the Eigen values m_i of moment tensor given by equation (2), where T means the transpose. In the major couple or double-couple solutions, one principal axis (T, B, P) of the related seismic source corresponds to each eigenvector of the moment tensor. T, B and P indicate the tension, null, and pressure axis, respectively. A moment tensor can be written as (Jost and Herrmann, 1989)

$$\mathbf{M} = [a_1 \ a_2 \ a_3] \text{diag}(m_i) \begin{bmatrix} a_1^T \\ a_2^T \\ a_3^T \end{bmatrix} \tag{5}$$

The Equation (5) is identical to the equation (2), and this equation is based on the orthonormality of the eigenvectors. The middle term on the right hand side of (5) is the diagonalized moment tensor (M'). The diagonalized moment tensor can be rewritten as

$$\mathbf{M}' = \text{diag}(m_i) = \text{diag}(\bar{m}) + \text{diag}(m_i^*) \tag{6a}$$

$$\mathbf{M}' = \bar{m} I + \text{diag}(m_i^*) \quad , \bar{m} = \frac{1}{3}(m_1 + m_2 + m_3) \tag{6b}$$

$$, m_i^* = m_i - \bar{m}$$

where I is the identity matrix and \bar{m} indicates the average of the trace of the moment tensor. The equations (6) show the general moment tensor decomposition which is decomposed into the isotropic part and the deviatoric part. The first term on the right hand side in

(6a) describes the isotropic part of moment tensor. The isotropic part is the monopole component of the seismic source, and it characterizes the volume change in the source. Also the second term is the deviatoric part of moment tensor. This represents the shear motion in the source. As to contribution rates in the source of these equivalent body forces, these can be calculated from the following equation (Jost and Herrmann, 1989)

$$\varepsilon = \frac{|m_{\min}^*|}{|m_{\max}^*|} \tag{7}$$

where ε is a parameter changing in intervals 0 and 0.5. It only represents the deviatoric component because of being calculated from purely deviatoric eigenvalues. If ε is equal to zero, the seismic source will be pure double-couple (DC). If ε is equal to 0.5, the source will represent a pure compensated linear vector dipole (CLVD). Alternatively, the percentages of DC can be calculated from $(1-2\varepsilon)*100$. Furthermore, if the calculation of the percentages of contribution of the force components to all seismic sources are required, the Eigen value representing the isotropic part is also considered.

A complete moment tensor can be written as the superposition of an isotropic part, a DC component and a CLVD component, too. Equation (8) shows an algebraic expression that gives the decomposition of the moment tensor in dyadics (Jost and Herrmann, 1989).

$$M = \frac{1}{3}(m_1 + m_2 + m_3)I + m_3^*(1-2F)(a_3a_3 - a_2a_2) + m_3^*F(2a_3a_3 - a_2a_2 - a_1a_1),$$

$$F = -m_1^*/m_3^* \tag{8}$$

As seen from Equation (8), mathematically an isotropic component is characterized by a tensor in the diagonal matrix form. Elements of the main diagonal are equal to each other. Consequently, this component has a physical property which applies equal force to each direction in focus of interest. Figure 1, schematically, shows the equivalent force components. The double-couple sources represent the extension and compression forces which are perpendicular and of equal strength with each other (Equation (8), Figure 1). The CLVD sources, however, are composed of three dyadics, one of which has opposite direction and is weighted two times more than the others (Equation (8), Figure 1).

By using the representation theorem for seismic sources the observed displacement at an arbitrary position (x) at the time (t) due to a distribution of equivalent body forces (f_j) in a source region is;

$$u_k(x, t) = \int_{-\infty}^{+\infty} \int_V G_{kj}(x, t; \bar{r}, \bar{t}) \cdot f_j(\bar{r}, \bar{t}) \cdot d^3r \cdot dt \tag{9}$$

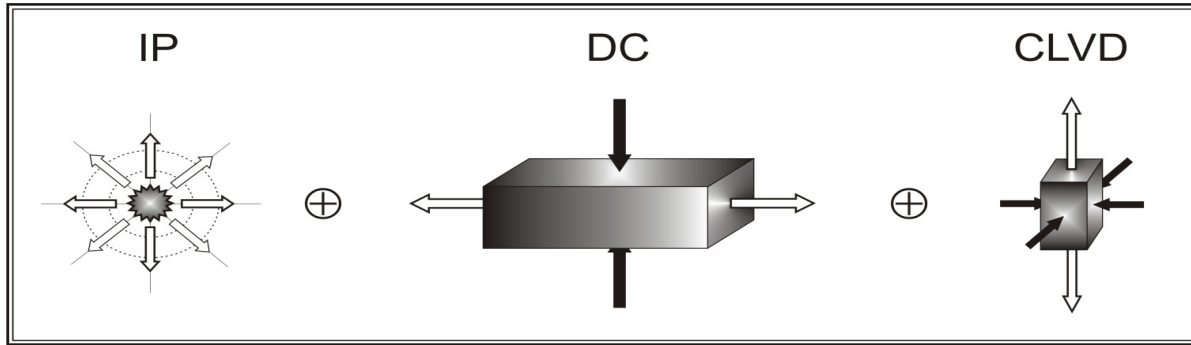


Figure 1. Schmatically view of the equivalent body forces formed a seismic source. IP, DC, CLVD stands isotropic part, double-couple, and compensated linear vector dipole, respectively. ⊕ indicates the superposition process.

where (G_{kj}) are the components of the Green's function, and (r, \bar{t}) are coordinates of source point (Jost and Herrmann, 1989; Bullen and Bolt, 1985; Kennett, 1983; Hartzell et al., 1978; Geller, 1976). The subscript k indicates the component of the displacement. Hence, the observed displacement is;

$$u_k(x, t) = [G_{kj,i} * s(\bar{t})] m_{ij} \tag{10}$$

where $*$ denotes the temporal convolution, and $s(\bar{t})$ is source time function. m_{ij} are constant representing the components of the second rank seismic moment tensor. Then, generally, the observed displacement in matrix form (Jost and Herrmann, 1989; Jackson and Mckenzie, 1988; Bullen and Bolt, 1985) is;

$$u = Gm \tag{11}$$

This seismogram is a linear combination of the seismic moment tensor and the Green's function. The linearity between the Green's function elements and the moment tensor was first used by Gilbert (1973) for moment tensor inversion. Green's function is the impulse response of the medium between source and receiver.

If the Green's function representing the medium is known, seismic moment tensor can be inverted from the seismogram. This kind of parameterization gives us a set of linear equations. Then, linear inverse theory can be applied to solve this problem. It can be performed either in time or frequency domain. This is called "the linear moment tensor inversion". The linear moment tensor inversion is estimated by six independent moment tensor components.

As a result of the decomposition each elementary moment tensor obtained from decomposition procedure represents corresponding force component. The equivalent forces can be determined from an analysis of the Eigen values and Eigen vectors of the moment tensor. The moment tensor can be decomposed into an

isotropic and deviatoric component (Fitch et al., 1980; Jost and Herrmann, 1989), or a major and minor double couple (Ben-Menahem and Singh, 1981; Kanamori and Given, 1981; Jost and Herrmann, 1989), or an isotropic part (IP) and double couple (DC) and compensated linear vector dipole (CLVD) (Knopoff and Randall, 1970; Ben-Menahem and Singh, 1981; Jost and Herrmann, 1989). Besides a complete moment tensor can be the superposition of an isotropic component and three vector dipoles (or three CLVD's or three double couple, Ben-Menahem and Singh, 1981; Jost and Herrmann, 1989). The Eigen vectors corresponding to each eigenvalues give the principal axes of source mechanism.

SEISMIC SOURCE MODELS

General seismic source

It represents the most general arbitrarily orientated seismic source. General seismic source is composed of both isotropic component and deviatoric component. The isotropic component is a part which represents volume variation of source. This component is characterized by an inward or outward pressure hoop. The deviatoric component is a part which represents shear dislocation of source. In other words, the deviatoric component is a piece that describes the dislocation component of source. That is to say, it is the non-volumetric part of source. Figure 2 shows such a seismic source. This source has an isotropic part, two strike-slip faults, two vertical faults, and a reverse fault. The isotropic component in this model is assumed as an explosion (Figure 2a). However, deviatoric component is composed of five differently orientated elementary sources (Figure 2b, c, d, e, f). The five elementary sources concerned are characterized by five elementary faults. Two of them are differently orientated strike-slip faults (Figure 2b, c) while the other two of them are again differently orientated vertical-dip slip faults (Figure 2d, e), and the last one is 45°-dip slip

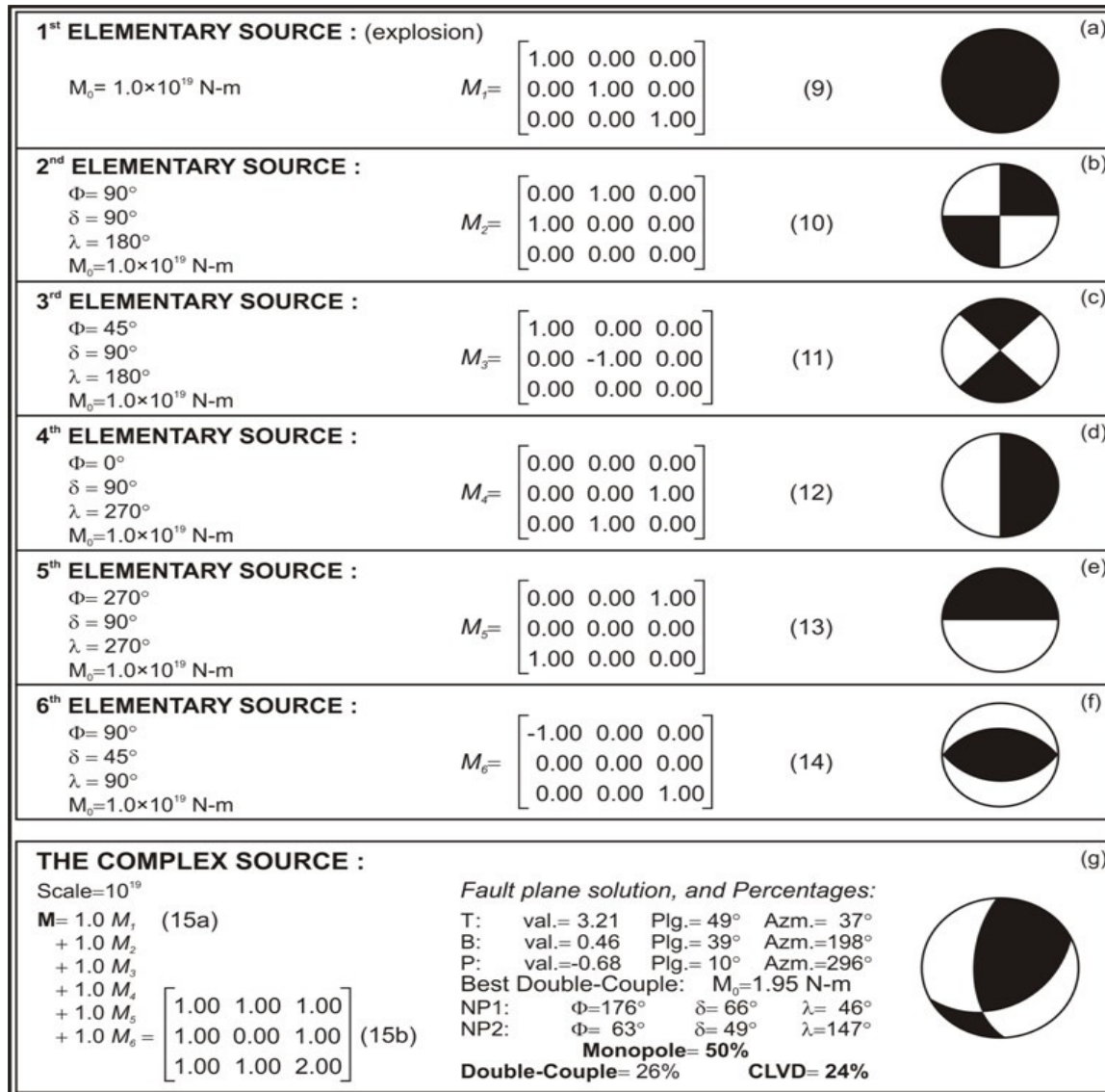


Figure 2. General seismic source and its elementary sources. Φ , δ , λ and M_0 indicates the strike, dip, slip and scalar seismic moment, respectively. M_i is elementary moment tensors. M is the complex moment tensor. Dark quadrants in the mechanism diagrams correspond to the compressional areas in the free surface. The representations are lower hemisphere, equal-area projections on the focal sphere. “val.,” “Plg.” and “Azm.” abbreviations correspond to the Eigenvalue, plunge and azimuth for the axes T, B, P.

reverse fault (Figure 2f). So, scalar seismic moments of elementary sources are equal and $M_0 = 10^{19}$ N-m is for all. Consequently, an arbitrarily orientated general seismic source is produced by a total of six elementary sources. The necessary parameters of these elementary sources such as physical and orientation parameters are given in Figure 2a, b, c, d, e, f. Moment tensor elements representing these elementary sources are also shown by equations (9), (10), (11), (12), (13) and (14) in Figure 2a, b, c, d, e, f respectively. Moment tensor elements describing the complex source composed of superposition of six elementary moment tensors are illustrated in Figure 2g. These elementary sources

provide equal contribution to the generation of the complex source because of having equal weight constants (c.f. Equation (15a) in Figure 2g). Major couple solution of complex source implies the characteristic properties of all elementary sources more. This is a very interesting case. *Major couple solution of complex source defined by calculating complex moment tensor, as seen from Figure 2g, shows a reverse faulting that has (NP1: $\Phi = 176^\circ$, $\delta = 66^\circ$, $\lambda = 46^\circ$; NP2: $\Phi = 63^\circ$, $\delta = 49^\circ$, $\lambda = 147^\circ$) orientation and minor strike-slip component.* In addition, as for equivalent body forces generating the complex source, the calculated complex moment tensor has a monopole component (isotropic part: IP) of 50%, a

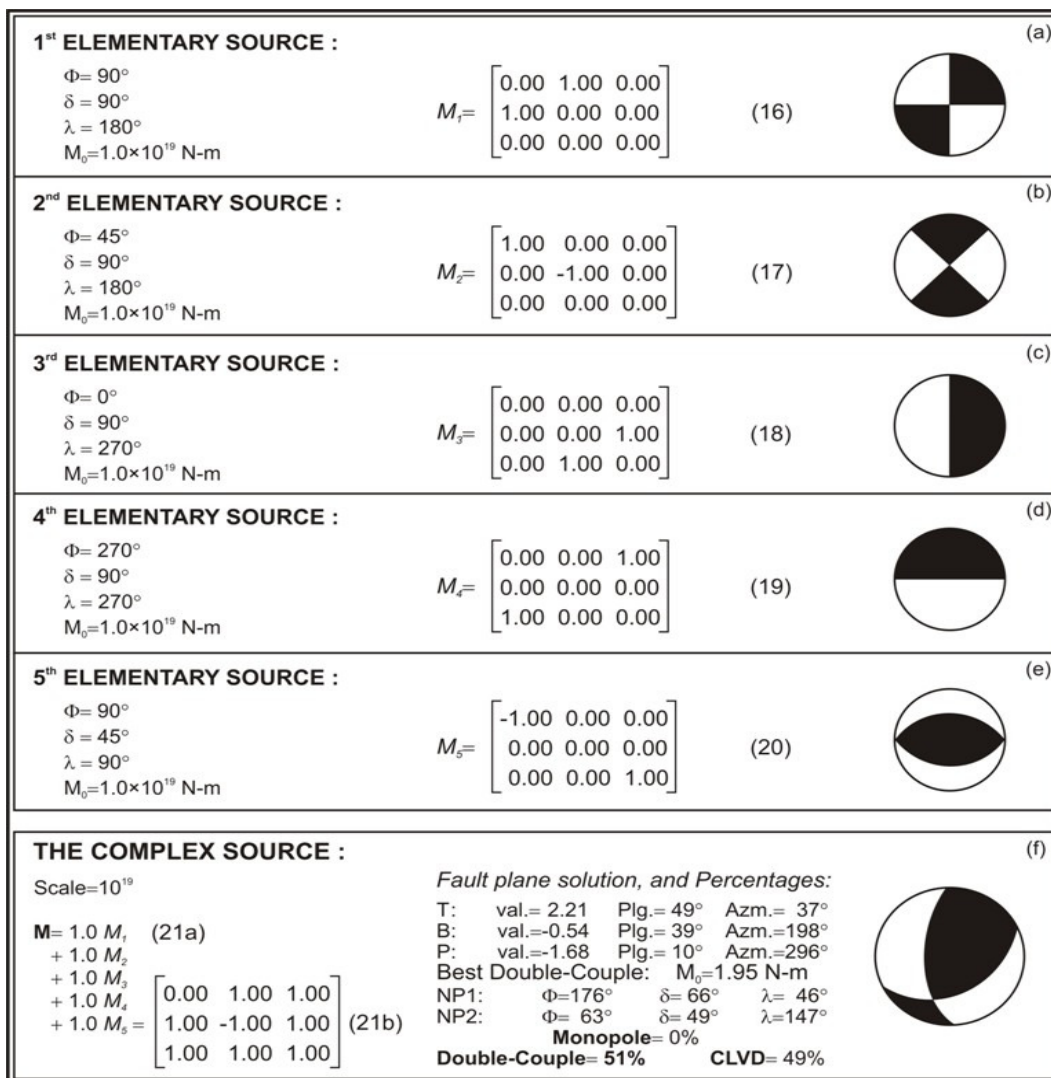


Figure 3. Deviatoric seismic source and its elementary sources. Φ , δ , λ and M_0 indicates the strike, dip, slip and scalar seismic moment, respectively. M_i is elementary moment tensors. M is the complex moment tensor. Dark quadrants in the mechanism diagrams correspond to the compressional areas in the free surface. The representations are lower hemisphere, equal-area projections on the focal sphere. "val.", "Plg." and "Azm." abbreviations correspond to the Eigenvalue, plunge and azimuth for the axes T, B, P.

double-couple (DC) component of 26%, and a compensated linear vector dipole component of 24%. Contribution rates of DC and CLVD components in deviatoric part are 51 and 49%, respectively. According to these percentages, general seismic source, first of all, shows a source character producing volumetric change and also characterizes a nondouble-couple force mechanism since the ratio of tensile contribution ($IP\% + CLVD\%$) was 74% whereas the percent DC ratio was 26%.

Pure deviatoric seismic source

This source type is generated only from deviatoric part.

What distinguishes it from the general seismic source is that it does not involve any isotropic components. Consequently, the pure deviatoric seismic source represents a shear dislocation, and it is a pure dislocation. The characteristic property of the moment tensor representing a deviatoric source is that the trace of the moment tensor is equal to zero. So, these sources characterize the earthquakes which are mostly deep and having the tectonic component. However, the earthquakes which occurred in shallow and flow mediums belong to this group, too.

Figure 3 shows a pure deviatoric seismic source. The elementary sources in Figure 3 are the same as elementary sources defining the deviatoric part of the

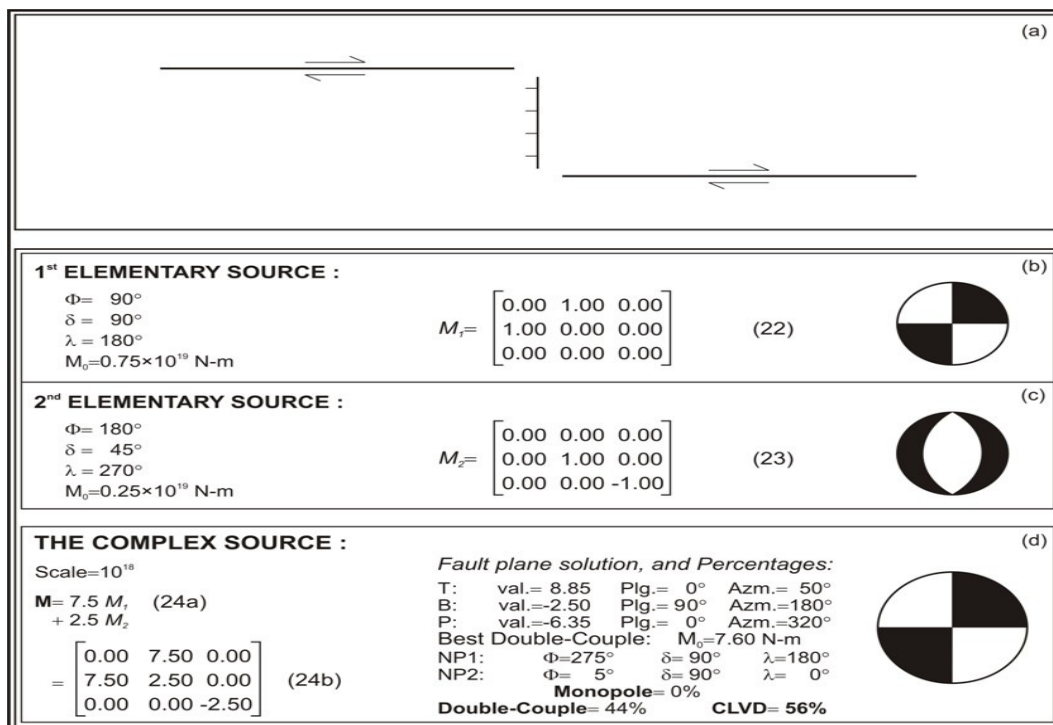


Figure 4. A complex seismic source characterizing the pull-apart rupture and its elementary sources. The top panel is a sketch map showing the modeling of a pull-apart tectonic structure. Ticks indicate the down thrown side. Φ , δ , λ and M_0 indicates the strike, dip, slip and scalar seismic moment, respectively. M_i is elementary moment tensors. M is the complex moment tensor. Dark quadrants in the mechanism diagrams correspond to the compressional areas in the free surface. The representations are lower hemisphere, equal-area projections on the focal sphere. "val.", "Plg." and "Azm." abbreviations correspond to the Eigenvalue, plunge and azimuth for the axes T, B, P.

general seismic source (Figure 2). For the elementary sources used, the orientation and physical parameters, the elementary moment tensor elements (Equations (16)-(20) in Figure 3), and the diagrams of fault mechanism are given in Figure 3. The resultant complex moment tensor is illustrated by Equation (21b) in the figure of interest. This is a deviatoric moment tensor. Its major-couple solution and tensor analysis results are located in Figure 3f. Fault plane solution of the calculated complex moment tensor is the same as in Figure 2g. The reason of this is hidden in the definition of fault plane solution since *the fault plane solution has a goal to determine the kinematics of shear phenomenon in earthquake source*. That is to say, the main criterion in fault plane solution is a shear activity. Consequently, it is valid for the same shear mechanism both at general seismic source (Figure 2) and pure deviatoric seismic source. As a result of this, it is unavoidable that the major couple solutions here are the same as those of theirs.

Then, the evaluation about the fault mechanism diagram relating to pure deviatoric seismic source will also be the same as the evaluation of general seismic source. However, complex moment tensor given by Equation (21b) in Figure 3f is different from Equation (15b) in Figure 2g. Also, this difference has been

generated from the lack of an isotropic component in the complex moment tensor given by Equation (21b). Furthermore, as seen from equivalent force percent in Figure 2g percent monopole, percent DC and percent CLVD were obtained as 0, 51, and 49%, respectively. These percents are the same as the proportions relating to non-volumetric component of the general seismic source. Its characteristic property is so: while it occurs as a part of source of interest in general seismic source, also in pure deviatoric seismic source, it rules the entire source.

That means, although pure deviatoric seismic source has not create any volumetric variation, it has represented approximately the nondouble-couple source character since 51 and 49% values are very close to each other. In other words, the pure deviatoric seismic source is not a DC dominant source, at least. This is a result which can be said easily.

Pull-apart tectonic structure

Pull-apart structures are the organization which is formed together by a strike-slip fault and a normal fault. Figure 4, schematically, shows such a tectonic structure. As

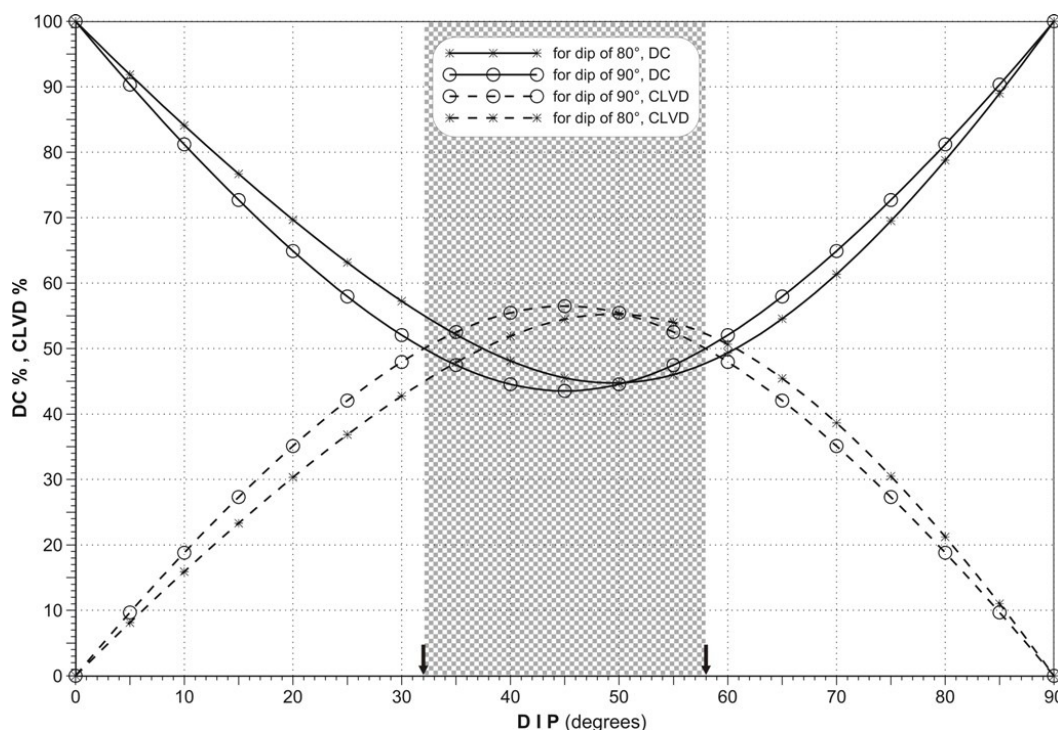


Figure 5. The response of pull-apart tectonic structure as a function of the dip of the normal fault component. The curves of “o” are the responses that assumed as 90° of dip of the strike-slip fault component in the system, and the curves of “*” are the responses that assumed as 80° of the dip. Solid and dashed lines shows the DC and CLVD contributions, respectively. The apsis axis displays the theoretical dip values of the normal fault component. Vertical arrows illustrate the nondouble-couple range for the dip values of normal fault.

seen from the figure, in this study, the strike-slip fault was assumed as right lateral whereas the normal fault is a 45° dip slip fault. Ticks of the normal fault in Figure 4a indicate downthrown side. The contribution rates in the organization of interest of these two faults are different from each other. From this point of view, in the generation of such a tectonic structure, it was supposed that strike-slip fault and normal fault contributed at the rates of 75 and 25%, respectively (Equation (24a)). Orientation parameters and scalar moments of the faults of interest, and the moment tensors (Equations (22), (23)) and fault mechanisms defining these elementary faults are given in Figure 4b, c. Equation (24b) defines the complex moment tensor characterized by the pull-apart system. As Figure 4d shows, the major couple solution of resultant complex moment tensor (Equation (24b)) is identical with those of the first elementary source since, as seen from Equation (24a) in Figure 4d, the first elementary source is dominant in the whole system. Consequently, the second elementary source with a contribution of 25% was able to create a deviation of approximately 5° only on the faulting strike. Likewise, by the analysis of the complex moment tensor shown in Figure 4d and given by equation (24b) in the same Figure, it appears that it has a DC component of 44% and

a CLVD component of 56%. The percent monopole of the complex source is 0%. Therefore, this system is a pure deviatoric system, too. However, it represents a nondouble-couple force mechanism.

In the pull-apart structure, there occurs an interesting result when the relation between strike-slip fault and normal fault is dealt with. Dip of the normal fault (δ_{ds}) has a determining property in this relationship. With regard to this, if the equivalent force components of a system formed by the contributions of the right lateral strike-slip fault and a normal dip-slip fault at certain rates are modelled as a function of the dip of a normal fault, the picture in Figure 5 is generated. This characterizes the response of the pull-apart structure associated with the equivalent force components as a function of δ_{ds} . When the parameters other than δ_{ds} are identical with those in Figure 4b, c, the curve of symbol “o” in Figure 5 shows the variation of the equivalent force components of the pull-apart tectonic structure as a function of δ_{ds} . In Figure 5, analogy line is for DC, dashed line is for CLVD. In the characteristic points (32, 50) and (58, 50), the contribution rates of DC and CLVD components are equal to each other as fifty-fifty. For $\delta_{ds}=45^\circ$, DC and CLVD contributions are 44 and 56%, respectively. Away from these points, DC contribution is increased although

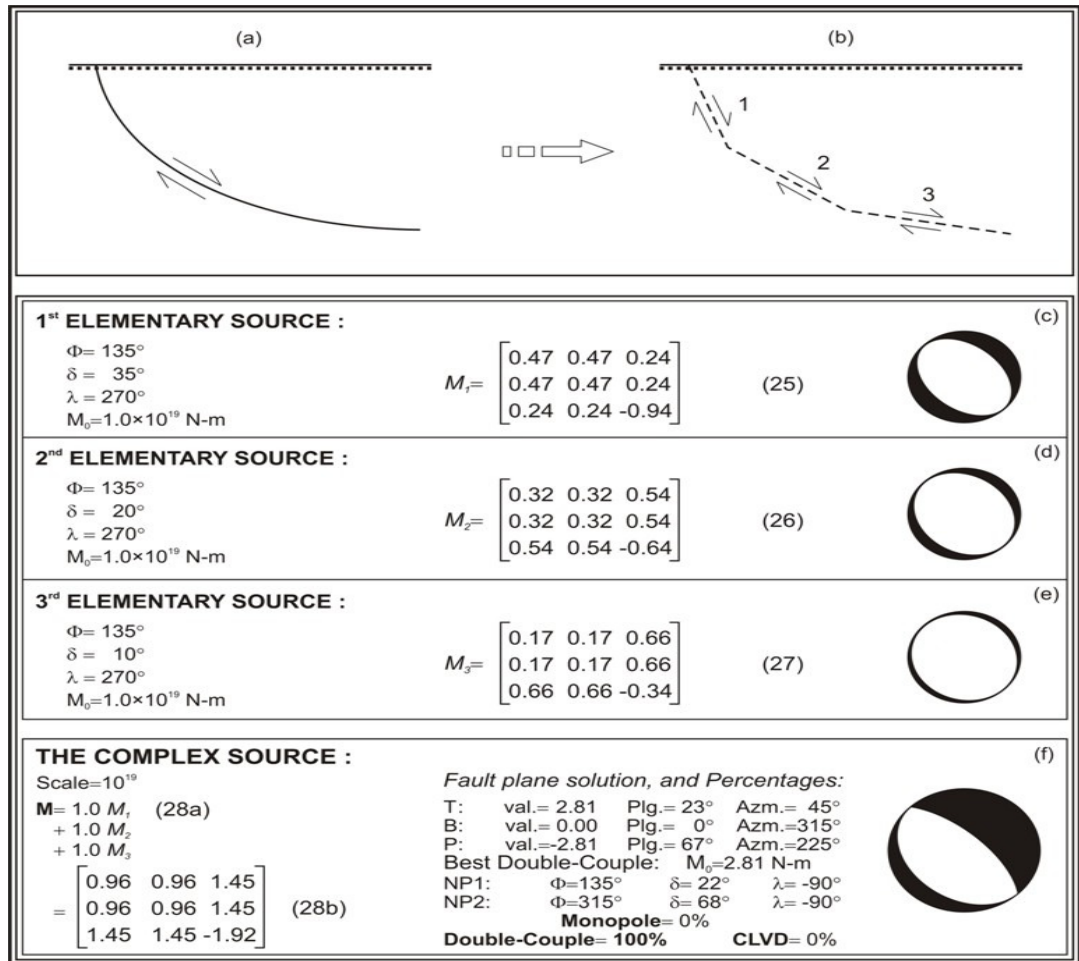


Figure 6. A complex seismic source characterizing the listric normal fault model and its elementary sources. (a) Sketch map showing the listric normal fault. (b) Sketch map showing the modeling of a listric normal fault. Numbers shows the fault segments used in the process of modeling. Φ , δ , λ and M_0 indicates the strike, dip, slip and scalar seismic moment, respectively. M_i is elementary moment tensors. M is the complex moment tensor. Dark quadrants in the mechanism diagrams correspond to the compressional areas in the free surface. The representations are lower hemisphere, equal-area projections on the focal sphere. "val.", "Plg." and "Azm." abbreviations correspond to the Eigenvalue, plunge and azimuth for the axes T, B, P.

CLVD contribution is decreased. In the event that δ_{ds} is smaller than 32 or greater than 58, this system turns into a DC dominant character.

To summarize the figure, in the event that the dip of the normal fault is between 32° and 58°, it is observed to exhibit a nondouble-couple force character of the system. Outside this range, the tectonic structure of interest has gone towards a DC dominant character in terms of the specific speed. The curve of symbol "*" in Figure 5 shows the response of system again in the same terms where dip of strike-slip fault component (δ_{ss}) is 80°. In this case, while δ_{ss} ranges between 38° and 61°, the system of interest is being nondouble-couple. Consequently, if we consider that the dip range guarantees the nondouble-couple force mechanism of the system, to say that the normal fault component has a dip in between 38° - 58°

means that the pull-apart tectonic structure characterizing the system is a nondouble-couple (Figure 5). If we change the strike of normal fault generated by the pull-apart system by 180°, the range is likely to be 32° - 58°. In short, the system is a nondouble-couple in the dip interval about 20° concerning normal fault. In addition, when the dip of strike-slip fault has a decreasing trend from 90° to 45°, the system is orientated towards a double-couple dominant character.

Listric normal fault

Seismological source modelling defining a listric normal fault is shown in Figure 6. When the listric normal fault is considered as a complex source modelling, the approach

Table 1. A chronological list of the Turkish earthquakes studied. m_b and M_0 represent the body wave magnitude and scalar seismic moment, respectively.

ID	Location area	Event (Year/Month/Day)	Origin Time (h/m/s)	Epicenter		m_b	M_0 ($\times 10^{25}$ dyne-cm)
				Latitude N($^\circ$)	Longitude E($^\circ$)		
1	Malatya	1964/06/14	121531.4	38.13	38.51	5.5	2.64
2	Demirci	1969/03/25	132134.2	39.25	28.44	5.5	2.49
3	Alaşehir	1969/03/28	014829.5	38.55	28.46	5.9	27.09
4	Karaburun	1969/04/06	034933.9	38.47	26.41	5.6	0.57
5	Gediz	1970/03/28	210223.5	39.21	29.21	6.0	141.40
6	Bingöl	1971/05/22	164359.3	38.85	40.52	5.9	34.73

in Figure 6b may be used. Figure 6a schematically shows the listric normal fault in nature. As can be seen from Figure 6b, we can separate the listric fault into infinite segments. Complex source is the superposition of the infinite segments. However, it requires finite segments since our calculation technique constrains. The listric fault in Figure 6a was assumed as the superposition of three segments in Figure 6b. According to this assumption, each segment is an individual fault and defines an elementary seismic source. For each elementary source, the parameters of interest and elementary moment tensors calculated from these parameters, and their fault mechanism diagrams are given in Figure 6c, d, e. The complex moment tensor generated by the superposition of these elementary moment tensors is represented by Equation (28a, b) in Figure 6f. This (28b) is a moment tensor characterized by the listric normal fault system. As seen from (28a), all elementary sources have equal weight. From the major couple solution of the complex moment tensor given by (28b), the fault mechanism in Figure 6f is obtained. This fault plane solution shows that there occurred no changes in the strike and slip of the resultant complex source in comparison to elementary sources and that, as for its dip, there is the average of the dips of elementary sources. By the analysis of the complex moment tensor, it is brought to light that the complex source is purely double-couple (Figure 6f). This result does not change even in the event that the listric normal fault is separated into more segments (>3). *It must be kept in mind that all interpretations made concerning listric normal fault have been made from the results based on the modelling where only a dip-based geometry is taken as the basis.*

MOMENT TENSOR INVERSION OF THE TURKISH EARTHQUAKES

Earthquakes selected from Western Anatolian region and East Anatolian Fault have been analyzed by using linear moment tensor inversion method. Table 1 illustrates these earthquakes. The seismograms have been

obtained from the 82 WWSSN type stations. Their epicentral distances range between about 30° and 90° . The seismograms have been digitized with the 0.5 and 1 s sample rates.

Dominant moment tensor elements of the teleseismic earthquakes have been investigated by linear moment tensor inversion method (Utku, 1997). The process of the calculation of moment tensor elements of the earthquakes have been performed in two steps. In the first step, the source parameters and source time function of the earthquake have been estimated using the waveform inversion method. In the second step, the best double couple solution of the moment tensor is estimated, and the moment tensor is decomposed. The dominant equivalent force of the moment tensor that represents the source, is determined by the decomposition process which gives the contribution rate of the equivalent body forces.

The results obtained from the inverse solution are given in Table 2 (Utku, 1997). These results show that two earthquakes from Eastern Anatolian Fault zone (14.06.1964, 22.05.1971) have a dominant double couple component. These two earthquakes have also isotropic components which represents an implosion type source. The four events from the west Anatolia region (25.03.1969, 28.03.1969, 06.04.1969, 28.03.1970) display tensile crack type source. The contribution rates of double couple are fairly low, with a rate of less than 30%. Figure 7 illustrates as schematically the equivalent body force components estimated using moment tensor inversion of the earthquakes studied (Utku, 1997). Topography and bathymetry data used in Figure 7 are from <http://edcdaac.usgs.gov/>. Figure 7 is a representation in proportion according to Table 2.

For the measure of the goodness of inversion process made both condition number and resolution matrix were used. Table 3 shows the condition numbers and resolution matrix elements related to the inversion results (Utku, 1997). According to these results, we can say that seismic moment tensor inversion was performed with high precision. As seen also from the Table 3, there is an over determined equation system in all of the solutions.

Table 2. The contribution ratios of equivalent body force components estimated using moment tensor inversion of the some Turkish earthquakes. IP, DC, CLVD stands isotropic part, double-couple, and compensated linear vector dipole, respectively. Φ , δ and λ indicates the strike, dip and slip, respectively.

ID	Event (Year/Month/ Day)	Moment tensor elements estimated (M_{xx} , M_{yy} , M_{zz} , M_{xy} , M_{xz} , M_{yz})	Scale (N-m)	Principal axes			Best double-couple			Contribution ratios of equivalent body forces (%)					Summation of Eigen values
				T	B	P	Φ ($^{\circ}$)	δ ($^{\circ}$)	λ ($^{\circ}$)	Source components			Deviatoric part		
				Plg.($^{\circ}$) Azm.($^{\circ}$)			NP1	NP2	Monopole	DC	CLVD	DC	CLVD		
1	1964/06/14	1.054, -1.573, -0.1516 $\cdot 10^{-3}$, 0.2393, -0.2287 $\cdot 10^{-3}$, -0.3637 $\cdot 10^{-4}$	10 ²⁰	0 185	90 3	0 95	320 230	90 90	180 0	14.7	64.5	20.8	76	24	-0.5192
2	1969/03/25	1.330, 2.347, 0.1090 $\cdot 10^{-3}$, -0.7756, -0.8364 $\cdot 10^{-6}$, 0.1126 $\cdot 10^{-3}$	10 ¹⁹	0 118	0 28	90 240	208 28	45 45	-90 -90	55.0	26.5	18.5	59	41	3.677
3	1969/03/28	1.845, 1.828, 0.1441 $\cdot 10^{-3}$, 0.3048 $\cdot 10^{-1}$, -0.2592 $\cdot 10^{-6}$, -0.1372 $\cdot 10^{-5}$	10 ²⁰	0 217	0 307	90 80	127 307	45 45	-90 -90	55.0	2.3	42.7	5	95	3.673
4	1969/04/06	1.720, 5.152, 0.1669 $\cdot 10^{-3}$, 0.4172, -0.9762 $\cdot 10^{-4}$, -0.2407 $\cdot 10^{-3}$	10 ¹⁸	0 263	0 173	90 43	173 353	45 45	-90 -90	69.6	17.4	13.0	57	43	6.872
5	1970/03/28	1.629, 2.050, 0.8722 $\cdot 10^{-4}$, 1.510, -0.1790 $\cdot 10^{-4}$, -0.1189 $\cdot 10^{-3}$	10 ²²	0 229	0 319	90 131	139 319	45 45	-90 -90	55.0	6.6	38.4	15	85	3.678
6	1971/05/22	-1.752, 1.192, -0.2982 $\cdot 10^{-5}$, 0.3599, 0.1338 $\cdot 10^{-3}$, 0.7174 $\cdot 10^{-4}$	10 ²⁰	0 83	90 308	0 173	128 218	90 90	180 0	15.7	64.7	19.6	77	23	-0.5601

Φ , δ , λ and M_0 indicates the strike, dip, slip and scalar seismic moment, respectively. M_i is elementary moment tensors. M is the complex moment tensor. "val.", "Plg." and "Azm." abbreviations correspond to the Eigen value, plunge and azimuth for the axes T, B, P.

Inversion for each earthquake had been performed by the unconstructed root mean square. Consequently, the condition numbers obtained are the small values used in order for the solution not to be difficult. As to relative errors of solution vectors, they are satisfactory (Table 3).

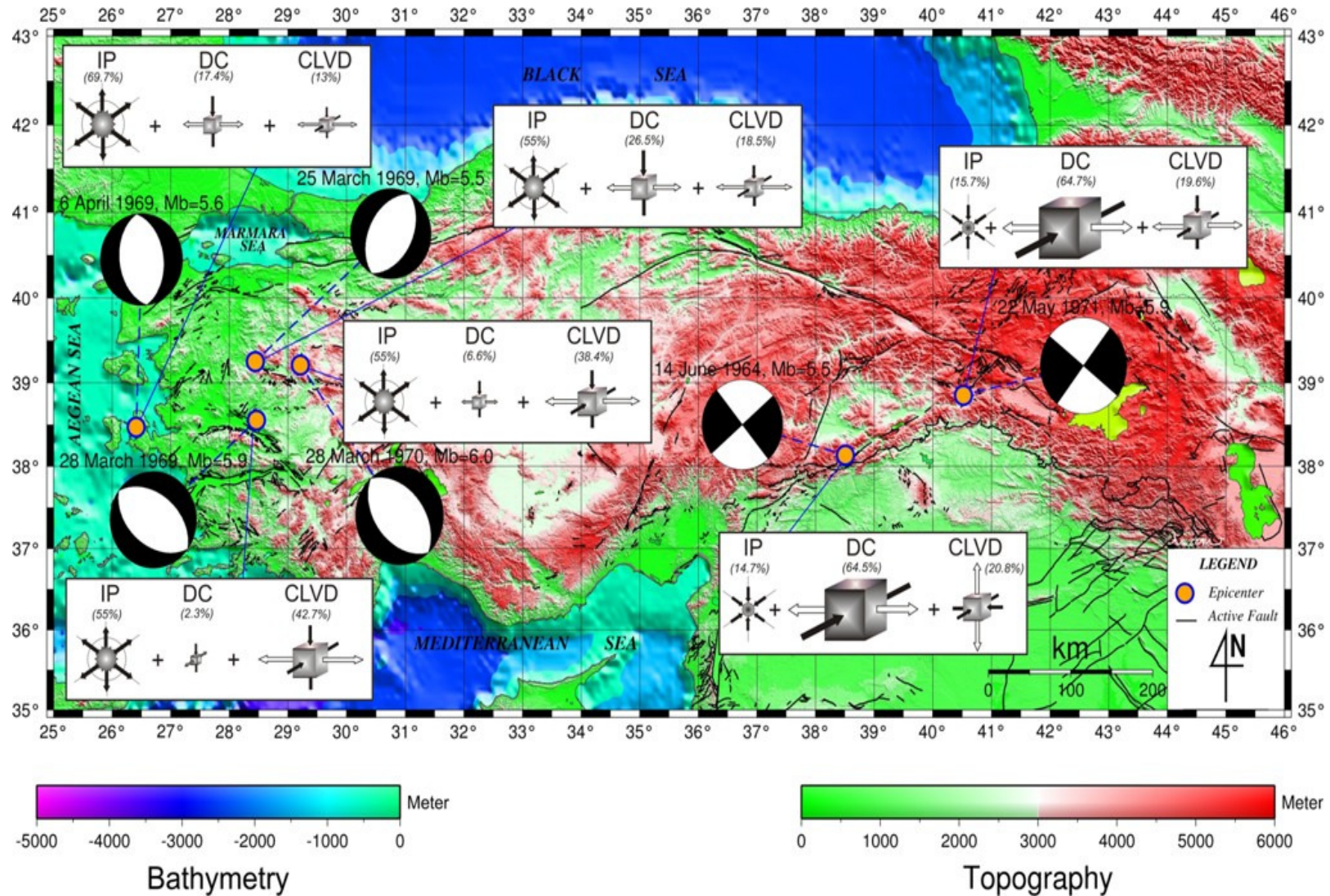


Figure 7. The equivalent body force components and best double-couple solutions of the some Turkish earthquakes estimated the moment tensor elements using moment tensor inversion. Fault mechanism diagrams belong to best double-couple solutions. Dark quadrants in the mechanism diagrams correspond to the compressional areas in the free surface. The representations are lower hemisphere, equal-area projections on the focal sphere. IP, DC, CLVD stands isotropic part, double-couple, and compensated linear vector dipole, respectively. The map was generated using GMT (Wessel and Smith, 2006). Topography and bathymetry data are from <http://edcdaac.usgs.gov/>. Active faults are modified from Şaroğlu et al. (1992).

Table 3. Solution sensitivities of the moment tensor inversions.

ID	Event (Year/Month/Day)	Observation number	Unknown parameter number	Solution method	Condition number ($\times 10^6$)	Under boundary of relative error*	Relative error of solution vector	Upper boundary of relative error*	Trace of Resolution Matrix
1	1964/06/14	8	6	Unconstrained R.M.S.	0.72	0.13×10^{-7}	1.094	4.50	0.17, 0.98, 0.79, 0.82, 0.26, 0.54, 0.51, 0.84
2	1969/03/25	11	6	Unconstrained R.M.S.	0.13	0.34	0.901	0.91	0.55, 0.02, 0.22, 0.36, 0.28, 0.25, 0.03, 0.54, 0.91, 1.05, 0.24
3	1969/03/28	21	6	Unconstrained R.M.S.	6.87	0.67×10^{-9}	0.999	67.43	0.004, 0.01, 0.13, 0.64, 0.004, 0.15, 0.24, 0.26, 0.02, 0.57, 0.40, 0.01, 0.17, 0.42, 0.03, 0.03, 0.41, 0.60, 0.59, 0.05, 0.16
4	1969/04/06	7	6	Unconstrained R.M.S.	7.82	0.44	0.551	18005.00	0.72, 0.67, 0.63, 0.24, 0.95, 1.00, 0.17
5	1970/03/28	15	6	Unconstrained R.M.S.	0.15	0.51×10^{-10}	0.327	0.33	0.09, 0.01, 1.28, 1.08, 0.02, 0.01, 0.95, 0.05, 0.08, 0.03, 0.008, 0.35, 0.09, 0.85, 0.61
6	1971/05/22	16	6	Unconstrained R.M.S.	0.16	0.44×10^{-2}	0.778	0.78	0.05, 0.003, 0.03, 0.34, 0.29, 1.25, 0.005, 0.0005, 0.50, 0.08, 0.03, 0.81, 0.03, 0.54, 0.47, 0.21

* Reachable value, R.M.S. stands for root mean square method.

The resolution matrixes have harmony with the error values.

Conclusions

Using time-independent seismic moment tensors, the complex seismic source modelling provides important information in terms of the knowledge of the active force types in different tectonic structures.

1. Although the general seismic source includes a minor double-couple component, essentially, it represents a tensile source.
2. Pure deviatoric seismic source is not at least a double-couple dominant source. That is to say, pure deviatoric seismic source does not always mean a dominant double-couple source.
3. Pull-apart tectonic structures represent the regions of many ruptures since they describe a nondouble-couple force mechanism. Therefore, it can be said that the shallow and intermediately deep earthquakes, the force component

- percentages of which are similar to those of pull-apart structure, belong to mediums of many ruptures.
4. In terms of the modelling conducted taking only a dip-based geometry as the basis, the listric normal faults are directed by a pure double-couple force mechanism.

The earthquakes in which, the moment tensor solutions was obtained, the source types in both the two regions seems to be coherent with the predominant tectonic kinematics of the regions.

The compressional regime in the Eastern Anatolia has been represented by thrust faults in the region. The isotropic components of the moment tensor solution indicate an implosive type volume change. The result may represent the thickening of the crust in the region where complex earthquakes take place. The tensile crack type sources are appropriated with the normal faults that dominate western Anatolia. These faults are the results of the extension in the region.

ACKNOWLEDGEMENTS

The author wish to acknowledge his Professor, his colleague, and the deceased humanist (Prof. Dr. Nezihi CANITEZ). Furthermore, the author is very grateful to Reviewers and Editor for their evaluations.

REFERENCES

- Aki K, Patton H (1978). Determination of seismic moment tensor using surface waves. *Tectonophysics*, 49: 213-222.
- Aki K, Richards PG (1980). *Quantitative Seismology Theory and Methods*, vol.I, II, W. H. Freeman and Co. San Francisco, USA, 932.
- Aki K, Bouchon M, Reasenber P (1974). Seismic source function for an underground nuclear explosion. *Bull. Seismol. Soc. Am.*, 64(1): 131-148.
- Backus G, Mulcahy M (1976). Moment tensors and other phenomenological descriptions of seismic sources-I. Continuous displacements, *Geophys. J. R. Astr. Soc.*, 46: 341-361.
- Backus GE (1977a). Interpreting the seismic glut moments of total degree two or less. *Geophys. J. R. Astr. Soc.*, 51(1): 1-25.
- Backus GE (1977b). Seismic sources with observable glut moments of spatial degree two. *Geophys. J. R. Astr. Soc.*, 51(1): 27-45.
- Batini F, Caputo M, Console R (1995). Focal Mechanism of Seismic Events with a Dipoler Component. *Annali di Geofisica*, XXXVIII(3-4): 373-384.
- Ben-Menahem A, Singh SJ (1981). *Seismic waves and sources*. Springer-Verlag New York Inc., USA, p. 1108.
- Bouchon M (1981). A simple method to calculate Green's functions for elastic layered media. *Bull. Seismol. Soc. Am.*, 71(4): 959-971.
- Buland R, Gilbert F (1976). Matched filtering for the seismic moment tensor. *Geophys. Res. Lett.*, 3(3): 205-206.
- Bullen KE, Bolt BA (1985). *An Introduction to the Theory of Seismology*. Cambridge University Press, USA, p. 499.
- Burridge R, Knopoff L (1964). Body Force Equivalents for Seismic Dislocations. *Bull. Seismol. Soc. Am.*, 54(6): 1875-1888.
- Day SM, Mclaughlin KL (1991). Seismic Source Representations for Spall. *Bull. Seismol. Soc. Am.*, 81(1): 191-201.
- Doornbos DJ (Editor) (1988). *Seismological Algorithms-Computational Methods and Computer Programs*. Academic Press, San Diego, Ca, USA, p. 469.
- Doornbos DJ (1982). Seismic Moment Tensors and Kinematic Source Parameters. *Geophys. J. R. Astr. Soc.*, 69: 235-251.
- Dziewonski AM, Gilbert F (1974). Temporal Variation of the Seismic Moment Tensor and the Evidence of Precursive Compression for Two Deep Earthquakes. *Nature*, 247: 185-188.
- Dziewonski AM, Chou TA, Woodhouse JH (1981). Determination of Earthquake Source Parameters from Waveform Data for Studies of Global and Regional Seismicity. *J. Geophys. Res.*, 86(B4): 2825-2852.
- Dziewonski AM, Woodhouse JH (1983a). An experiment in systematic study of global seismicity: Centroid-moment tensor solutions for 201 moderate and large earthquakes of 1981. *J. Geophys. Res.*, 88(B4): 3247-3271.
- Dziewonski AM, Woodhouse JH (1983b). Studies of the seismic source using normal-mode theory. In: Kanamori H, Boschi E (eds) *Earthquakes: Observation, Theory and Interpretation*, North-Holland Publishing Company, Amsterdam, New York, Oxford, pp. 45-137.
- Dziewonski AM, Franzen JE, Woodhouse JH (1984). Centroid-moment tensor solutions for January-March 1984. *Phys. Earth Planet. Interiors*, 34: 209-219.
- Ekström G, Dziewonski AM (1985). Centroid-moment tensor solutions for 35 earthquakes in western North America (1977-1983). *Bull. Seismol. Soc. Am.*, 75(1): 23-39.
- Fitch TJ, Mccowan DW, Shields MW (1980). Estimation of the seismic moment tensor from teleseismic body wave data with applications to intraplate and mantle earthquakes. *J. Geophys. Res.*, 85(B7): 3817-3828.
- Fitch TJ, North RG, Shields MW (1981). Focal depths and moment tensor Representations of shallow earthquakes associated with the Great Sumba earthquake. *J. Geophys. Res.*, 86(B10): 9357-9374.
- Frohlich C (1990). Note concerning non-double-couple source components from slip along surfaces of revolution. *J. Geophys. Res.*, 95: 6861-6866.
- Frohlich C (1995). Characteristics of well-determined non-double-couple earthquakes in the Harvard CMT catalog. *Phys. Earth Planet. Interiors*, 91: 213-228.
- Frohlich C, Riedesel MA, Apperson KD (1989). Note concerning possible mechanisms for non-double-couple earthquake sources. *Geophys. Res. Lett.*, 16: 523-526.
- Geller RJ (1976). Body force equivalents for stress-drop seismic sources. *Bull. Seismol. Soc. Am.*, 66(6): 1801-1804.
- Gilbert F (1970). Excitation of the normal modes of the earth by earthquake source. *Geophys. J. R. Astr., Soc.*, 22: 223-226.
- Gilbert F (1973). Derivation of source parameters from Low-frequency spectra. *Phil. Trans. R. Soc., A* 274: 369-371.
- Gilbert F, Dziewonski AM (1975). An application of normal mode theory to the retrieval of structural parameters and source mechanisms from seismic spectra. *Phil. Trans. R. Soc., A* 278: 187-269.
- Hartzell SH, Frazier GA, Brune JN (1978). Earthquake modeling in a homogeneous half-space. *Bull. Seismol. Soc. Am.*, 68(2): 301-316.
- Herrmann RB (1975). A student's guide to the use of P and S wave data for focal mechanism determination. *Earthquake Notes*, 46(4): 29-40.
- Herrmann RB, Wang CY (1985). A comparison of synthetic seismograms. *Bull. Seismol. Soc. Am.*, 75(1): 41-56.
- <http://edcdaac.usgs.gov/>, June 1, 2005.
- Jackson J, Mckenzie D (1988). The relationship between plate motions and seismic moment tensors, and the rates of active deformation in the Mediterranean and Middle East. *Geophys. J.*, 93: 45-73.
- Jost ML, Herrmann RB (1989). A student's guide to and review of moment tensors. *Seismol. Res. Lett.* 60(2): 37-57.
- Kanamori H, Given JW (1981). Use of long-period surface waves for rapid determination of earthquake-source parameters. *Phys. Earth Planet. Interiors*, 27: 8-31.
- Kanamori H, Given JW (1982). Use of long-period surface waves for rapid determination of earthquake source parameters: 2. Preliminary determination of source mechanisms of Large earthquakes ($M_s > 6.5$) in 1980. *Phys. Earth Planet. Interiors*, 30: 260-268.
- Kanamori H, Boschi E (eds) (1983). *Earthquakes: Observation, Theory and Interpretation*. North-Holland Publishing Company, Amsterdam, p. 608.
- Kennett, BLN (1983). *Seismic wave propagation in stratified media*. Cambridge University Press, USA, p. 342.
- Kikuchi M, Kanamori H (1991). Inversion of complex body waves-III. *Bull. Seismol. Soc. Am.*, 81(6): 2335-2350.
- Knopoff L, Gilbert F (1959). Radiation from a strike-slip fault. *Bull. Seismol. Soc. Am.*, 49(2): 163-178.
- Knopoff L, Randall MJ (1970). The compensated Linear-Vector dipole: a possible mechanism for deep earthquakes. *J. Geophys. Res.*, 75(26): 4957-4963.
- Kubas A, Sipkin SA (1987). Non-double-couple earthquake mechanisms in the Nazca Plate subduction zone. *Geophys. Res. Lett.*, 14: 339-342.
- Langston CA (1981). Source inversion of seismic waveforms: The Koyna, India, earthquakes of 13 September 1967. *Bull. Seismol. Soc. Am.*, 71(1): 1-24.

- Langston CA, Helmberger DV (1975). A procedure for modeling shallow dislocation sources. *Geophys. J. R. Astr. Soc.*, 42: 117-130.
- Lay T, Wallace TC (1995). *Modern Global Seismology*, Academic Press, New York, p. 521.
- Madariaga R (1983). Earthquake Source Theory: A Review. In: Kanamori H, Boschi E (eds) *Earthquakes: Observation, Theory and Interpretation*, North-Holland Publishing Company, Amsterdam-New York-Oxford, pp. 1-44.
- Marshall GA, Stein RS, Thatcher W (1991). Faulting geometry and slip from co-seismic elevation changes: The 18 October 1989, Loma Prieta, California, earthquake. *Bull. Seismol. Soc. Am.*, 81(5): 1660-1693.
- McCowan DW (1976). Moment tensor representation of surface wave sources. *Geophys. J. R. Astr. Soc.*, 44: 595-599.
- McKenzie DP (1972). Active tectonics of the Mediterranean Region. *Geophys. J. Royal Astr. Soc.*, 30: 109-185.
- Mendiguren JA (1977). Inversion of surface wave data in source mechanism studies. *J. Geophys. Res.*, 82(5): 889-894.
- Müller G (2001). Volume Change of Seismic Sources from Moment Tensors. *Bull. Seismol. Soc. Am.*, 91(4): 880-884.
- Nábělek JL (1984). Determination of earthquake source parameters from inversion of body waves. PhD dissertation, Massachusetts Inst. Technol. USA.
- Nakanishi I, Kanamori H (1982). Effects of lateral heterogeneity and source process time on the linear moment tensor inversion of long-period Rayleigh waves. *Bull. Seismol. Soc. Am.*, 72(6): 2063-2080.
- Nakanishi I, Kanamori H (1984). Source mechanisms of twenty-six large, shallow earthquakes ($M_s > 6.5$) during 1980 from P-wave first motion, and long-period Rayleigh wave data. *Bull. Seismol. Soc. Am.*, 74: 805-818.
- Ohtsu M (1991). Simplified Moment Tensor Analysis and Unified Decomposition of Acoustic Emission Source: Application to *in situ* Hydrofracturing Test. *J. Geophys. Res.*, 96(B4): 6211-6221.
- Randall MJ (1964a). On the mechanism of earthquakes. *Bull. Seismol. Soc. Am.*, 54(5): 1283-1289.
- Randall MJ (1964b). Seismic energy generated by a sudden volume change. *Bull. Seismol. Soc. Am.*, 54(5): 1291-1298.
- Randall MJ (1966). Seismic radiation from a sudden phase transition. *J. Geophys. Res.*, 71(22): 5297-5302.
- Randall MJ (1971). Elastic multipole theory and seismic moment. *Bull. Seismol. Soc. Am.*, 61(5): 1321-1326.
- Randall MJ, Knopoff L (1970). The mechanism at the focus of deep earthquakes. *J. Geophys. Res.*, 75(26): 4965-4976.
- Sipkin SA (1982). Estimation of earthquake source parameters by the inversion of waveform data: Synthetic waveforms. *Phys. Earth Planet. Interiors*, 30: 242-255.
- Sipkin SA (1986). Interpretation of non-double-couple earthquake mechanisms derived from moment tensor inversion. *J. Geophys. Res.*, 91(B1): 531-547.
- Strelitz RA (1978). Moment tensor inversions and source models. *Geophys. J. R. Astr. Soc.*, 52: 359-364.
- Strelitz RA (1980). The fate of the downgoing slab: A study of the moment tensors from body waves of complex deep-focus earthquakes. *Phys. Earth Planet. Interiors*, 21: 83-96.
- Strelitz RA (1981). The interpretation of moment tensor inversions. In: Husebye EC, Mykkeltveit S (eds) *Identification of seismic sources-Earthquake or Underground Explosion*, D. Reidel Publishing Company Hingham, Mass, 273-275.
- Stump BW, Johnson LR (1977). The determination of source properties by the linear inversion of seismograms. *Bull. Seismol. Soc. Am.*, 67(6): 1489-1502.
- Stump BW, Johnson LR (1982). Higher-degree moment tensors the importance of source finiteness and rupture propagation on seismograms. *Geophys. J. R. Astr. Soc.*, 69: 721-743.
- Şaroğlu F, Emre Ö, Kuşçu İ (1992). Active fault map of Turkey. General Directorate of Mineral Research and Exploration, Ankara, Turkey.
- Şengör AMC, Canitez N (1982). The North Anatolian fault, Alpine Mediterranean Geodynamics. *AGU, Geodyn. Ser.*, 7: 205-216.
- Vasco DW, Johnson LR (1988). Inversion of waveforms for extreme source models with an application to the isotropic moment tensor component. In: McEvelly TV, Johnson LR (eds) *Regional Studies with Broadband Data*, Report No.1, Air Force Geophysics Laboratory, AFGL-TR-88-0131.
- Wang CY, Herrmann RB (1980). A numerical study of P-, SV-, and SH-wave generation in a plane layered medium. *Bull. Seismol. Soc. Am.*, 70(4): 1015-1036.
- Ward SN (1980). Body wave calculations using moment tensor sources in spherically symmetric, in homogeneous media. *Geophys. J. R. Astr. Soc.*, 60: 53-66.
- Ward SN (1983). Body wave inversion: Moment tensors and depth of oceanic intraplate bending earthquakes. *J. Geophys. Res.*, 88: 9315-9330.
- Wessel P, Smith WHF (2006). *The Generic Mapping Tools (GMT) version 4.1.4 Technical Reference & Cookbook*, NOAA/NESDIS.
- Utku M (1997). *Sismik Moment Tansör Ters Çözümüyle Türkiye Depremlerinin Analizi* (The analysis of major earthquakes in Turkey using the seismic moment tensor inversion). Unpublished PhD dissertation, İstanbul Technical University, Turkey.